In Situ Measurement of Electrical Behavior of Metal/Oxide System During Zirconium Oxidation at 850 °C

Juan Carlos Pereira, Philippe Breuil, Jean-Paul Viricelle

In situ measurement of electrical behavior of metal /oxide system during zirconium oxidation at 850°C.

J.C. Pereira, P. Breuil and J-P. Viricelle
Mines Saint-Etienne, Univ Lyon, CNRS, UMR 5307 LGF, Centre SPIN, F-42023, Saint-Etienne, France.

Corresponding author : J-P. Viricelle, viricelle@emse.fr

ABSTRACT

Comprehension of oxidation processes under the influence of an external polarization is still a challenge, despites numerous past studied. In this study, thermogravimetric analysis technique coupled with in-situ application of an electric voltage was used to investigate oxidation of zirconium. First technical challenge was to modify thermobalance to integrate polarization equipment without perturbation of measurement and of oxidation behavior. Surprisingly, the oxidation rate was found to remain independent on the applied voltage, despite a large range of applied potential +/-200 Volts. Modeling of oxidation rates according to diffusion mechanism combined with investigation of polarization curves of the metal/oxide/electrode system have shown that a high electrical resistance appears at the oxide/electrode interface, even with addition of an intermediate gold layer. This resistance prevents from generating sufficient voltage drop through the oxide layer (>10 V), necessary to modify the kinetics. Nevertheless, meaningful electrochemical properties using analogy with solid oxide fuel cell have been observed, allowing to propose a comprehensive approach of oxidation phenomena under polarization.

KEYWORDS: oxidation, kinetics, diffusion, thermogravimetry, polarization, zirconium.

DECLARATIONS

Conflicts of interest
The authors declare that they have no conflict of interest.

Availability of Data and Material
Raw data of the present study will be made available on demand.

Code Availability
Not applicable.

1. Introduction

Influence of electric field or polarization on the kinetics of metals oxidation has been studied for many years. Recently, this topic has attracted much attention because of its applications on the fabrication of nanodevices systems [1], the development of solid oxide fuel cell technology (SOFC) [2] and the corrosion protection of materials operating at ultra-high temperature (UHT) [3]. However, it has not been possible to reach a consensus to explain

various experimental results depending on the properties of the metal/oxide system, the testing temperature and the electrical conditions.

Some authors, such as Jorgensen [4],[5], Hinze [6], Kawamura et al. [2], and Saunders et al. [3] have shown that the oxidation is slowed down when the metal/oxide interface is positively polarized with respect to the oxide/gas interface and it is accelerated when the metal/oxide interface is negatively polarized. However, Ritchie et al. [7] have suggested that it is possible to obtain the opposite result depending on the testing temperature for nickel oxidation. Meanwhile, Roy et al. [8] have found that two modes of electric current application (interrupted or uninterrupted) can produce contrary effects on the oxidation kinetics of copper. On the other hand, Lawless et al. [9] show that oxidation of stainless steel 304 exhibits a deceleration with the application of electrical voltage, regardless of the polarization direction. Other studies from Uhlig et al. [10] and Lawless et al. [9] lead the conclusion that electric voltage has no effect on the oxidation rate of Cu and Ni respectively, but in both cases, no explanation was proposed. More recently, N. Parkansky et al. investigated copper oxidation [11] and zinc oxide growth [12] in applied electric field and they have observed significant effects on both kinetics and oxide structure. Finally, A. V. Shishkin et al. [13] have studied the effect of electric field on oxide layer structure for zirconium oxidation in H_2O, CO_2 and H_2O/CO_2 supercritical fluids at 823K. In their conditions, when Zr is oxidized in CO_2 in the presence of the electric field, a 12-fold increase in the rate of zirconium oxidation is registered. The explanation is that the electric field modifies the oxidation mechanism with or without zirconium carbonate formation.

Based on previous results, and driven by the need for new techniques to study oxidation mechanisms under polarization, the goal of this study is to provide deeper information on such mechanism, developing coupling of thermogravimetric analysis with in-situ polarization, and using current-voltage polarization curves of the studied system. To this end, zirconium has been selected for this study, as its oxidation kinetics (in normal conditions, without external polarization) has been extensively studied, as detailed hereafter.

Generally, regardless of the atmosphere (oxygen, air or steam), at atmospheric pressure and temperatures between 500 and 1200°C, the oxidation of zirconium (or zirconium alloys) initially evolves with the thickness of oxide layer following parabolic-like kinetics, according to diffusion mechanism: oxidation is limited by oxygen diffusion through the oxide layer. Then, when the formed oxide is not able to heal the cracks induced by the oxide growth, the metal is no more protected and suffers from degradation according to a linear kinetic, indicating an interface reaction limiting step. This particular transition from parabolic to linear kinetics is commonly referred to as “breakaway” [14-18]. In this study, the effect of polarization is tested during oxidation before the breakaway, where diffusion process governs the oxidation kinetics.

In such conditions, the general admitted mechanism for zirconium oxidation is the following, according to equations (1) to (7), using Kröger-Vink notations [15-17]:

Reactions at the oxide/oxygen external interface (EI)

- Dissociative oxygen adsorption:

$$O_2 + 2s \rightleftarrows 2O\text{–s} \quad (1)$$

- Incorporation of oxygen anion in the oxide:

$$O - s + V_O^{\circ\circ} + 2e' \rightleftarrows O_O^X + s \quad (2)$$

Diffusion through the oxide layer

- Oxygen anion: $O_O^X \quad (IE) \rightarrow \; O_O^X \quad (II)$ (3)
- Oxygen vacancy: $V_O^{\circ\circ} \quad (II) \; \rightarrow \; V_O^{\circ\circ} \quad (IE)$ (4)
- Electrons: $e' \quad (II) \; \rightarrow \; e' \quad (IE)$ (5)

At the metal/oxide internal interface (II)

- Oxygen dissolution in Zr: $Zr_{Zr(metal)}$ + O → Zr(O) (6)
- Zr oxidation and vacancy formation:

$$Zr_{Zr(metal)} \rightleftarrows Zr_{Zr}^X + 2V_O^{\circ\circ} + 4e' \quad (7)$$

Where, s is an adsorption site on the zirconia surface (ZrO_2), $V_O^{\circ\circ}$ is an oxygen vacancy, O_O^X and Zr_{Zr}^X are oxygen anion and zirconium cation, respectively in zirconia lattice, e' are free electrons in the solid, Zr(O) is a solid solution of oxygen in zirconium. EI and II, respectively "External Interface" and "Internal Interface", allow to define accurately where the reaction occurs.

This overall mechanism distinguish 3 reaction areas: at the oxide/oxygen external interface (EI), oxygen in incorporated in the oxide layer via dissociative adsorption (Eq. 1) and reaction of adsorbed species with oxygen vacancy to produce oxygen anions (Eq. 2). Electrons and oxygen vacancies are produced at the metal/oxide internal interface (II) by the oxidation reaction of zirconium (Eq. 7). Then, they diffuse through the oxide layer from II to IE (Eq. 4 and Eq. 5), while oxygen anions has a counter-diffusion form IE to II (Eq. 3). Another additional reaction that occurs is oxygen dissolution in zirconium (Eq. 6).
In regards of the diffusion of charged species inside ZrO_2 oxide layer, it may be expected that the application of an external electric field or polarization during the oxidation may affect the reaction kinetics.

2. Experimental

2.1 Samples

A sheet of zirconium 99,2% pure (ZR000310) provided by Goodfellow was used in this study. The samples were cut to 7 mm x 7 mm for thermogravimetry tests. The thickness is equal to 0,5 mm, which enables to minimize the mass gain due to the edges compared to that due to the plane faces. The bare plates were cleaned in acetone and dried before each experiment. For some experiments, a porous layer of gold, approximately 0,5 µm thick, was applied on

both sides of the sample by sputtering, while masking the sample slices to avoid deposition on this area and further electrical short circuit.

2.2 Thermogravimetric analysis with *in-situ* application of electric voltage

The experimental procedure consists in recording continuously the weight change of the sample which is subjected to constant conditions of temperature, gas flow and an applied electric voltage. To this end, a modified non-symmetrical thermobalance Setaram CS32 (weighing accuracy ±0,1 µg) connected to an electrical power supply was used. The traditional platinum suspension has been replaced by a double-drilled alumina support rod (400 mm in length and 3 mm in diameter) allowing the passage of two platinum wires (250 µm in diameter) from the sample holder to the thermobalance head. At the top end of the suspension, each platinum wire is welded to a copper wire (80µm in diameter), which is fastened to an electrically isolated support on the base plate of the balance and subsequently connected to the external power source. This reduction in diameter with thin flexible copper wire allows to ensure the electrical connection without distortion of balance readout (weight measurement). This result was a technological challenge and the modification has been validated by comparing thermogravimetric curves measured using the traditional platinum suspension and the new designed one including electrical connections (but without applied polarization) : similar weight gains versus time (kinetic curves) were registered using both type of suspensions (not shown here).

On the sample side, a platinum grid, connected to one of the wires, plays the role of electrode. The second wire is welded directly onto the metal plate, which serve as the second electrode (Fig. 1). As it is known that zirconium oxidation proceeds via an internal growth of the oxide layer (internal diffusion of oxygen anion through the oxide layer, Eq.3) [14-17], it has been checked by SEM observations that this second electrical connection, directly to the metal, is not be damaged during oxidation. The contact between the platinum wire and Zr metal is maintained during the whole duration of oxidation experiment which allows to apply a constant voltage once a continuous oxide layer has grown. Moreover, this unsymmetrical configuration allows the application of the electrical voltage only to one oxide layer (between Zr metal and platinum grid, right oxide side in Fig.1), while the second oxide layer remains outside the electric circuit and serves as a "reference oxide" to compare the oxidation (oxide thickness) with and without polarization. It must be noted, that the applied voltage (V) also named “polarization” in the paper is the voltage applied between Zr metal and the platinum grid electrode. Thus, it does not correspond to the voltage across the oxide layer if significant contact resistances appear at the different interfaces.

The electrical power supply connected to the platinum wires is a 2635B Keithley multimeter-SourceMeter. It can operate either as a voltage source and measure the current, or as a current source and measure the voltage. Switching from one mode to another is done automatically if the current (voltage source mode) or voltage (current source mode) apparatus threshold is exceeded. The maximum current is 1.5 A up to 20 volts and 100 mA between 20 and 200 volts.

Oxidation experiments were conducted under 20% O_2 - 80% He gas mixture at 850°C and atmospheric pressure. The total flow rate was fixed at ambient to 5 $NL.h^{-1}$, which was sufficient to avoid kinetics limitations from the reactive gas supply. The temperature was raised at a rate of 14°C.min^{-1} up to 850 °C. When this temperature is reached, polarization is applied. The oxidation kinetics and electrical behavior are monitored under isothermal and isobaric conditions during several hours.

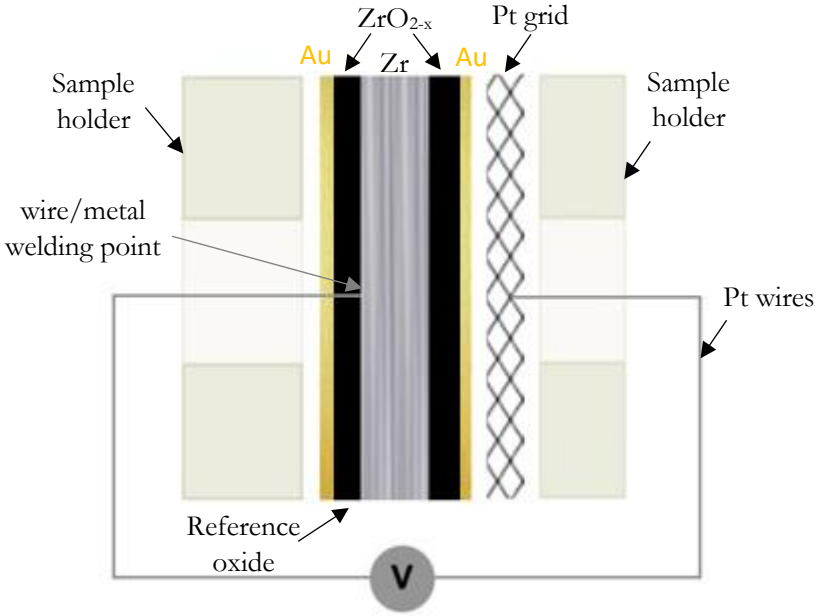

Fig. 1. Schematic representation of the sample holder cross-section and electrical connections (with optional porous sputtered gold layer depending on samples).

2.3 Polarization curves

Polarization (voltage-current) curves enables to investigate the electrical behavior under oxidation of the metal substrate/oxide/electrode assembly which can be considered more or less as an electrochemical cell (Zr /ZrO_{2-x}/Pt), with ZrO_{2-x} acting as a mixed conductor (electronic and ionic), by electrical analogy. However, contrary to an electrochemical cell, the electrolyte is not under equilibrium and goes under oxidation, with increasing thickness. Polarization curves were measured at different oxidation times during the isothermal bearing. The current was applied from -0.1 up to +0.1 A with a constant rate (0.9 mA/sec). For each curve, the measurement was repeated 3 times (3 cycles from -0.1 to +0.1 A) to assess the reproducibility of the results.

3. Results and discussion

3.1 Ionic oxygen flow and expected effect of polarization

In parabolic regime the oxidation rate of zirconium, limited by oxygen diffusion according to mechanism previously described in 1-Introduction is proportional to the flow of oxygen ions

($J_{O^{2-}}$) through the oxide layer. This flow may described according from the Nernst-Einstein law, using the usual linear diffusion equation, Eq. (8) with two main driving forces [19]. The first one is a chemical force due to the gradient of oxygen concentration $\frac{dC_{O^{2-}}(x)}{dx}$ in the oxide layer (J_D chemical diffusion term in Eq. (8)) and the second one is an electric force caused by the difference in electric potential $\frac{d\varphi(x)}{dx}$ existing between the metal/oxide interface and the oxide/gas interface (J_M electric migration term in Eq. (8))

$$J_{O^{2-}} = \underbrace{-D_{O^{2-}} \frac{dC_{O^{2-}}(x)}{dx}}_{J_D \text{ Chemical diffusion}} \underbrace{- \mu_{O^{2-}} \frac{d\varphi(x)}{dx} C_{O^{2-}}(x)}_{J_M \text{ Electric migration}} \quad (8)$$

From this relation, it is possible to determine the order of magnitude of the external electric voltage (φ) necessary to significantly affect the ion oxygen flow and consequently the oxidation rate. To this end, the values of the diffusion coefficient ($D_{O^{2-}}$) and the oxygen concentration at the interfaces were taken from the literature.

There is a wide range of diffusion coefficient values at 850°C (between 10^{-14} and 10^{-8} cm²/s) [20-25] which varies depending on the heat treatment of zirconium alloy, its chemical composition and all the experimental conditions. The value reported by Kasperski et al. ($D_{O^{2-}}$=7.1x10^{-9} cm²/s) was chosen, because it is the most recent study on zirconium alloys oxidation with experimental conditions similar to ours [25]. The oxygen mobility ($\mu_{O^{2-}}$) was calculated from the Einstein-Smoluchowski relation (Eq. 9)

$$\mu_{O^{2-}} = \frac{|z|.F.D_{O^{2-}}}{R.T} \quad (9)$$

where z is the electric charge of oxygen ions (z=2), F the Faraday constant, R the universal gas constant, T the temperature and $D_{O^{2-}}$ is the diffusion coefficient of O^{2-} ions in zirconia.

A linear O^{2-} diffusing species concentration profile with constant external and internal interfaces concentrations over the oxidation duration in diffusion regime was taken as hypothesis. Zirconium oxide is assumed to be stoichiometric at its external surface and the oxygen concentration at the metal/oxide interface is fixed by the equilibrium between the ZrO_2 and α-Zr(O) phases. Such phases are known to be formed during zirconium oxidation [15, 17, 26] This internal concentration is taken from the calculated Zr-O binary phase diagram proposed by Ma and coworkers [26], which gives 5.65 at% vacancies concentration at 850°C. To simplify the calculation, the concentration of oxygen ions $C_{O^{2-}}(x)$ used in the J_M term was an average value between the concentrations at the external and internal interfaces of the oxide layer.

Fig. 2 shows the two terms of oxygen flow J_D and J_M and the total J, calculated from Eq. 8 and previous values, as a function of the applied voltage, for a 20 µm thick oxide layer. The chemical diffusion flow J_D does not depend on the applied voltage while the electric migration

flow J_M increases linearly with the electrical voltage, for a constant thickness, accordingly to Eq. 8. At 10 V, both fluxes are equal ($J_M \approx J_D$). As J_M and J_D are both inversely proportional to the oxide layer thickness (Eq. 8), this equivalence at 10V does not depend on oxidation time. For higher voltage, J_M becomes higher than J_D, suggesting that the polarization may significantly affect the oxidation kinetics, regardless of the progress of the reaction. Thus, an acceleration or a slowing of the corrosion rate should occur, according to the direction of polarization, under these conditions (U>10 V).

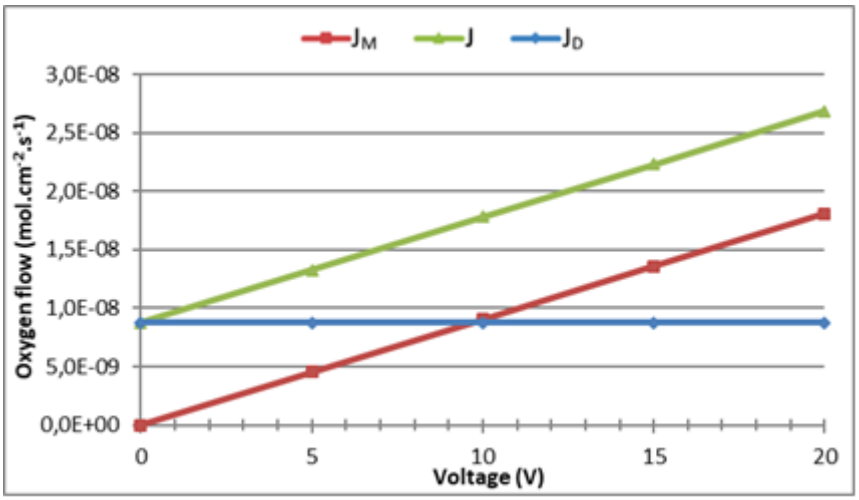

Fig. 2. Calculated oxygen ion flow in 20 µm thick zirconia layer as a function of voltage applied during oxidation of zirconium at 850°C: in blue the chemical diffusion term (J_D), in red the electric migration term (J_M) and in green the total flux (J).

To illustrate such hypothesis, diagrams of the cross-section of an oxidized sample are shown in Fig.3 with either positive (Fig. 3(a)) or negative (Fig. 3(b)) polarization of the external oxide/gas interface. As explained previously, the “reference oxide” (left oxide side in Fig. 1) should not be influenced as it remains out of the electrical circuit. In case of positive polarization (Fig. 3(a)), the electric field created between these two interfaces opposes the internal diffusion of oxygen ions (reaction 3), resulting theoretically in a thinner oxide layer. Opposite phenomena should occur for a negative polarization (Fig. 3 (b)), accelerating the oxidation kinetics and forming a thicker oxide layer. Such expected influence of the electrical polarization has also been proposed by K. Kawamura et al. [2] for Cr_2O_3 oxide formation on SOFC interconnect.

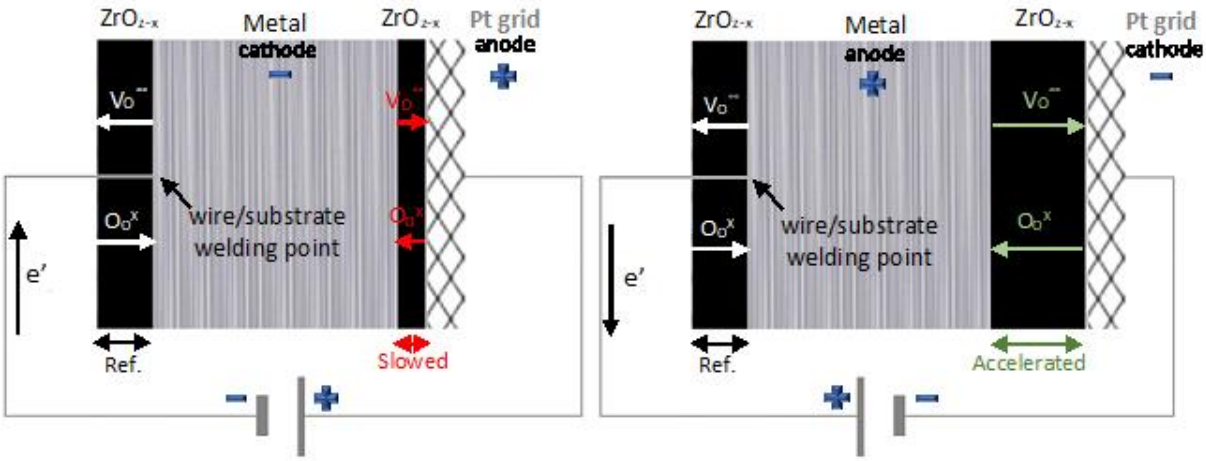

(a) (b)

Fig. 3. Expected diagram of the cross-section of an oxidized sample under (a) positive and (b) negative polarization of the oxide/gas external interface.

3.2. Oxidation kinetics under polarization without gold layers

To begin this study, intermediate gold layers were not deposited on the samples. A first experimental part was carried out to check the influence of polarization on the oxidation kinetics. Fig. 4 shows the comparison of mass gain and oxidation rates (per unit area) of zirconium obtained without applied voltage, under +200 volts and under -200 volts. The three curves are similar showing parabolic-like kinetics with no significant effect on the corrosion rate. Hence, a first important conclusion is that, in present oxidations conditions, the sample remains under diffusion kinetic regime, and the breakaway transition defined in the introduction is not reached. The second key observation is the unexpected absence of polarization effect. The morphology of the sample oxidized during 4 hours under +200 V is shown in Fig. 5 as example. No difference in terms of thickness between the reference and polarized oxide layers is found (around 15 µm for both sides) .

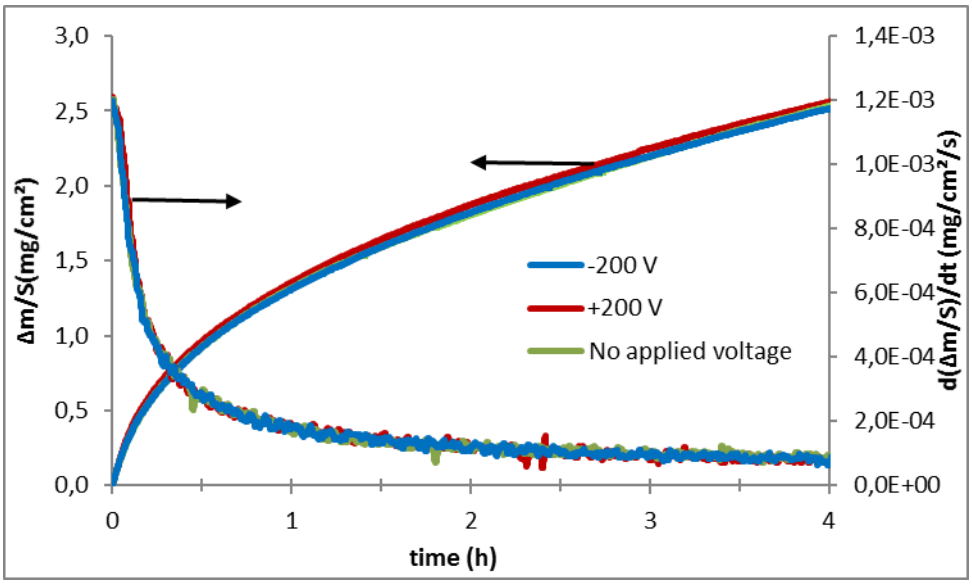

Fig. 4. Mass gain and mass gain rate as a function of time during oxidation of zirconium (no gold layer) at 850°C in 20%O_2-80%He mixture with +200 V (red curve), -200 V (blue curve) and no applied voltage (green curve).

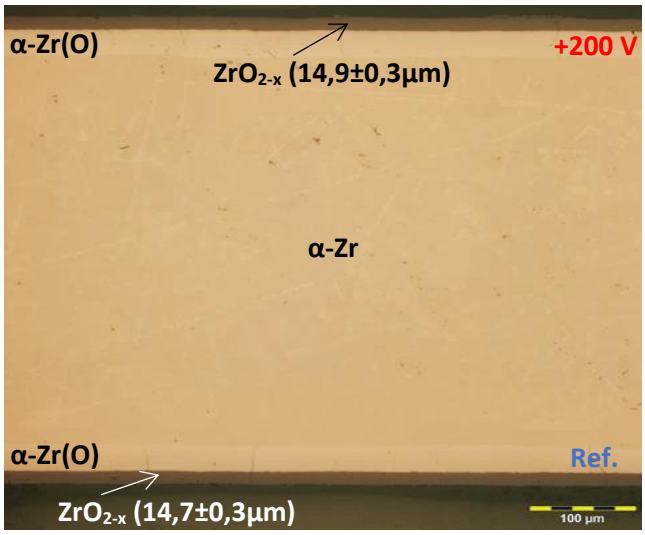

Fig. 5. Optical image of the cross-section of zirconium oxidized during 4h at 850°C in 20%O_2-80%He under +200 V applied voltage.

The thicknesses of the zirconia layers at different oxidation times of zirconium were also measured, to assess the effect of polarization on thinner oxide layers, where the applied electric field is higher (due to the lower thickness). The differences in thickness of the oxides formed without applied voltage, or with +200 volts or -200 volts, are not significant and confirm the absence of effect of the electric voltage on the corrosion kinetics, independently of the oxidation time studied (Table 1), contrary to expectations from diffusion flow calculation which has indicated that a significant effect should appear for polarization higher than 10V. (part 3.1).

Table 1. Thicknesses of oxide layers at different oxidation times of zirconium at 850°C without electric applied voltage, or with an applied voltage of +200 V and -200 V.

Oxidation time (h)	Thickness of the oxide layer (µm)		
	No Power Supply	Under +200 V	Under -200 V
1,3	5,5±0,4	6,0±0,4	5,3±0,6
2,3	9,6±0,2	9,5±0,4	9,8±0,3
3,0	11,2±0,4	11,1±0,4	11,6±0,4
5,0	14,7±0,5	14,5±0,5	14,8±0,5

3.3 Electric potential during oxidation without gold layers

The electric potential during zirconium oxidation at 850°C was measured experimentally, when there was no current in the external circuit. It is named open circuit potential (OCP). So, OCP is the open circuit potential measured experimentally across the system Zr/ZrO2/(gold)/Pt grid

electrode under oxidation, and not at equilibrium. Fig. 6 shows a sharp increase of OCP at 640°C during the temperature rise. Initial OCP increase reflects the formation of a continuous zirconia layer, thus switching from a metallic structure (Zr) to a metal/oxide one, with electrically insulation of the metal from the platinum grid. Then, after a peak just before the temperature stabilization, the potential remains constant at 1V regardless of the oxidation time and the thickness of the oxide layer.

It must be noted that the observed oscillations are due to an interference with the 50 Hz of the power supply and the data acquisition system with a sampling period of 20ms, and not to any physicochemical phenomena.

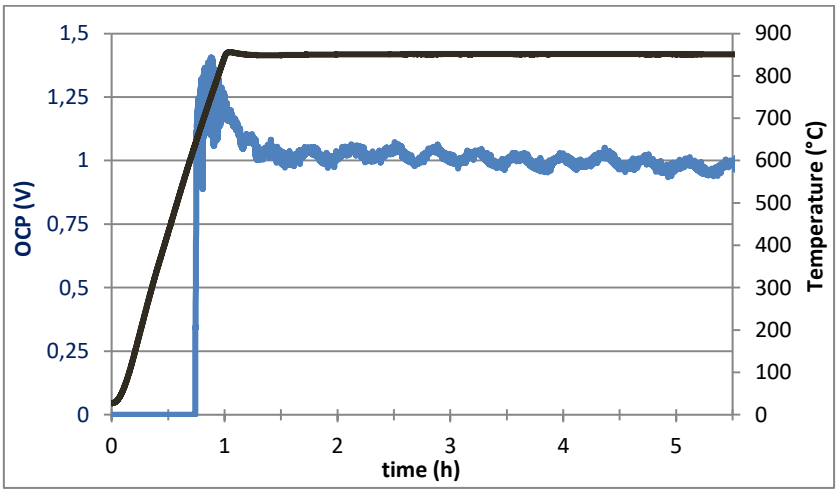

Fig. 6. Open circuit potential (OCP) measured across the system Zr/ZrO2/Pt grid electrode during zirconium oxidation in 20%O_2-80%He mixture at 850°C.

3.4 Oxidation current without gold layers

From an electrochemical point of view, in non-polarized condition (no power supply), the system metal/oxide/electrode during oxidation is similar to an electrochemical cell. The metal substrate behaves like an anode with oxidation reaction at the metal/oxide interface (reaction 7). The platinum grid in contact with the oxide plays the role of the cathode with the reduction of gaseous oxygen at the interface oxide/Pt (reaction 2). The zirconia layer can be assimilated to an electrolyte, behaving like a mixed conductor (ions and/or electrons). In open circuit condition (Fig. 7(a)), that means, in "conventional" oxidation mode, oxygen vacancies ($V_O^{\circ\circ}$) and electrons diffuse through the oxide layer from the metal to the oxide surface, with associated counter diffusion of O^{2-} ions (O_O^X of the oxide network). If an external “short-circuit” is made between the metal and the Pt grid (Fig. 7(b)), electrons produced by the oxidation reaction can be partially transported to the "cathode" through this preferential

pathway, while the zirconia layer is responsible of ionic conduction, acting as a solid electrolyte.

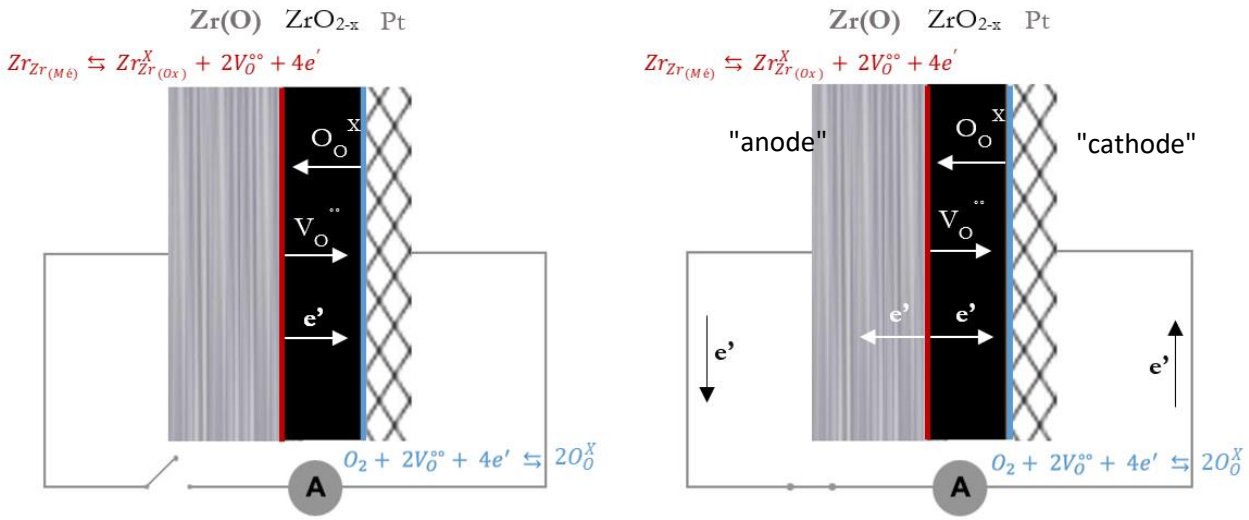

Fig. 7. Diagram of ionic and electronic transport (a) with open circuit and (b) closed circuit, during the oxidation.

Under short-circuit condition, the electronic current passing through the external circuit (I_{Ox}^{Ext}) was measured, to be compared with the total electronic current resulting from the oxidation reaction (I_{Ox}). This latter is calculated from the experimental oxidation rate according to Eq. 10:

$$I_{Ox} = n.F.\frac{1}{2}.\frac{d\Delta m}{dt}.\frac{1}{M} \quad (10)$$

where n is the number of electrons per adsorbed oxygen atom (n=2), F is the Faraday constant in C/mol, M is the molar mass of atomic oxygen in g/mol (M=16) and $\frac{1}{2}\frac{d\Delta m}{dt}$ corresponds to the oxidation rate of a single face of the sample in g/s (the second face is not involved in the "electric process", even if the oxidation occurs symmetrically).

This current (I_{Ox}) is identical to the ionic current in absolute value and it only depends on the oxidation rate ($\frac{d\Delta m}{dt}$), which itself do not depend on polarization condition (Fig.4). However, depending on the electric configuration (open or closed circuit), I_{Ox} can be divided into two parts: the internal oxidation current (I_{Ox}^{Int}), corresponding to electron flow passing through the oxide layer, and the external oxidation current (I_{Ox}^{Ext}) corresponding to electron flow migrating via the external circuit. Thus, we have the relation (Eq. 11) between these different electronic currents.

$$I_{Ox} = \left|I_{Ox}^{Ext}\right| + \left|I_{Ox}^{Int}\right| \quad (11)$$

Fig. 8 shows the curve of the total oxidation current (I_{Ox}, green curve) of zirconium at 850°C, calculated from the oxidation rate (Eq. 10). I_{Ox} continuously decreases from 7.7 mA at the beginning of the isothermal bearing down to 0.7 mA after 4 hours of oxidation. In contrast, the maximum value of the current passing through the external circuit (I_{Ox}^{Ext} without Au, red

curve) is 2.2 µA and decreases to 0.7 µA at the end of the experiment. This low external current (nearly 1000 times lower than total current I_{Ox}) indicates that the majority of the electrons from oxidation reaction are transported through the oxide layer.

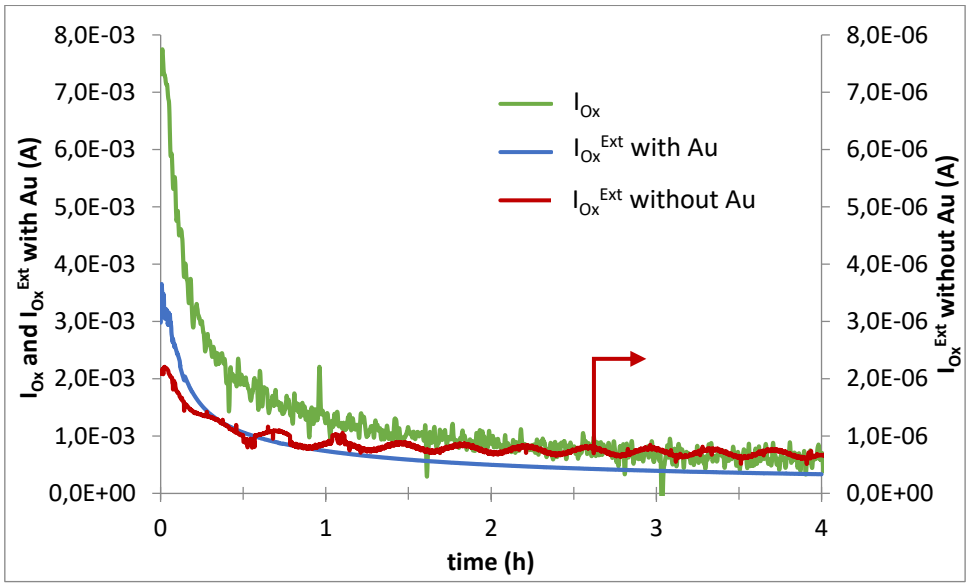

Fig. 8. Comparison of the calculated total oxidation current (I_{Ox}) and the measured external current (I_{Ox}^{Ext}, short circuit current) as a function of time, for the zirconium oxidation at 850°C with and without gold layers.

Therefore, this result induces that electronic resistance of the zirconia layer under oxidation is 1000 times lower than that of the external circuit, which nevertheless has negligible impedance, considering platinum wires and grid. Hence, to take into account this phenomenon, it is assumed that there is a high contact resistance (R_{cont}) at the interface between the Pt grid and the zirconia surface (similar to electrode polarization resistance). Under these conditions, we have a voltage divider and almost the entire electric potential drop occur across the contact resistance and not across the oxide layer, which explains why there is no effect of external electric voltage on the oxidation kinetics.

3.5 Oxidation of samples with gold layers

In order to eliminate or at least reduce the contact resistance between the Pt grid and the forming zirconia, a thin layer of gold was applied on the metal substrate before oxidation as shown in Fig.1. As the oxide grows on the internal interface (internal development) [14-17], the gold layer will remain on the surface of the oxide during oxidation, ensuring the direct contact with the Pt grid.

The first tests made with these sample were conducted to check that the gold layer does not affect the oxidation kinetics, without external polarization. Thermogravimetric experiments were conducted in the same conditions as previously. The curves are perfectly superimposable for both types of samples, similar to the ones in Fig. 4, indicating that gold layers are

sufficiently porous and do not disturb the oxidation kinetic of zirconium. Moreover, oxidation tests were also performed under external short circuit and under polarization.

Under short circuit conditions, kinetic curves were not modified. Hence the total oxidation current of the reaction (I_{Ox}), calculated from thermogravimetric measurement (Eq. 10) is the same with and without gold deposition. Concerning external current (I_{Ox}^{Ext}), it was measured like for previous samples without gold. In this case, I_{Ox}^{Ext} varies from 3.7 mA at the beginning of the oxidation down to 0.35 mA, which is much higher than the current measured without gold deposition, from 2.2 µA down to 0.7 µA (Fig. 8). This result shows that the gold thin layer allows to drastically reduce the "contact resistance" by a factor of 1000, thus validating our hypothesis of "contact resistance" betwen the oxide layer and the platinum grid. With gold layer, the ratio I_{Ox}/I_{Ox}^{Ext} is around 1.5 indicating that the contact resistance is now is 1.5 times that of the oxide layer (contrary to 1000 times higher without gold).

In such conditions, for polarization of samples with gold, we had to limit the current value to 100 mA. Indeed, given the low impedances encountered, this maximum value was necessary to keep the electrical power below a few hundred of mW to avoid sample heating by Joule effect. With such a current limitation, the maximum voltage that could be applied was around 4 V. We were able to calculate that the temperature rise due to Joule effect is then below a few °C, thus not modifying the kinetic.

In all cases, without polarization or with polarization under limited current (100mA, around 4V), oxidation kinetic was still the same. No difference of oxide layer thickness was observed from optical microscopy images, similarly to the ones reported in Table 1.

All these results prove that zirconium oxidation does not depend on the electronic transport, but it remains limited by the ionic oxygen diffusion through the oxide layer, regardless of the studied polarization conditions. For samples with gold, due to the current limitation required to avoid any overheating by Joule effect, the non-influence of the external polarization around 4V is a consistent result with our previous calculation (part 3.1) indicating that a minimum value of 10V is necessary to have a predominant effect of electrical migration flow (J_M, Eq.8).

3.6 Polarization curves

In order to deeper investigate the previous electrical behavior observed during oxidation, polarization curves were recorded. Fig. 9 shows a typical curve obtained after 4.5h at 850°C; the most notable aspects are the hysteresis and the non-ohmic behavior. These two characteristics were previously reported by M.Howlader et al [27] during the measurement of the electric conductivity of the zirconia resulting from the oxidation of Zircaloy-4 and Zircaloy-2 at 400°C. They attributed this behavior to a Schottky effect due to oxide/electrode contact having different work functions. The arrows shown in Fig. 9 correspond to the current scan direction. A non-ohmic curve is obtained during the growing scan (from -0.1 to 0.1A) while a near ohmic behavior is monitored during the decreasing scan (from 0.1 to -0.1A).

Similar responses were obtained with two different scanning rates (0.2 and 0.9 mA/sec) which indicates that the hysteresis is not caused by a kinetic effect. Thus, it may originate from the polarization of the oxidizing system at high current. To check this hypothesis, polarization curve was measured under a "short cycle" between -0.1 and 0.1 mA, previous one between -0.1 and 0.1 A being named hereafter "long cycle". Fig. 10 shows that the hysteresis in the short cycle has almost disappeared. In addition, a similar behavior is observed for both cycles in increasing scan condition. The quasi-ohmic behavior is only present during decreasing scan when a high current was applied (long cycle).

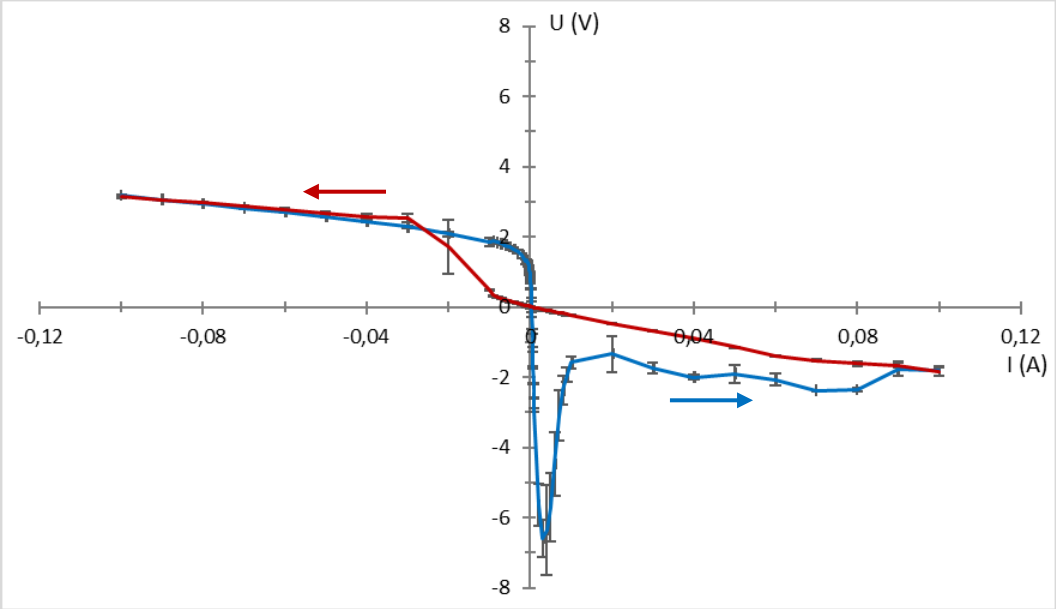

Fig. 9. Polarization curve of Zr with gold deposit after 4.5h oxidation under He-20%O_2 at 850°C. The arrows indicate the direction of current variation (0.9 mA/s).

To interpret polarization curves, three different zones are distinguished from Fig.10. Two zones, in the upper left quadrant (U>0 and I<0) and lower right quadrant (U<0 and I>0) correspond to a receptor mode of operation of metal/oxide system (Fig. 11). For the first quadrant called "negative reception zone" (I<0), the imposed external current goes in the same direction as the internal oxidation current (I_{Ox}^{Int}), that is from the external oxide/Au interface to the internal metal/oxide interface via the oxide layer. Hence, there is therefore no external oxidation current (I_{Ox}^{Ext} =0, I_{Ox} = I_{Ox}^{Int} from Eq. 11). This domain corresponds to a positive polarization of the oxide side electrode (Au-Pt), which was expected to be unfavorable to the oxidation of zirconium (Fig. 11(a) and Fig 3(a)).

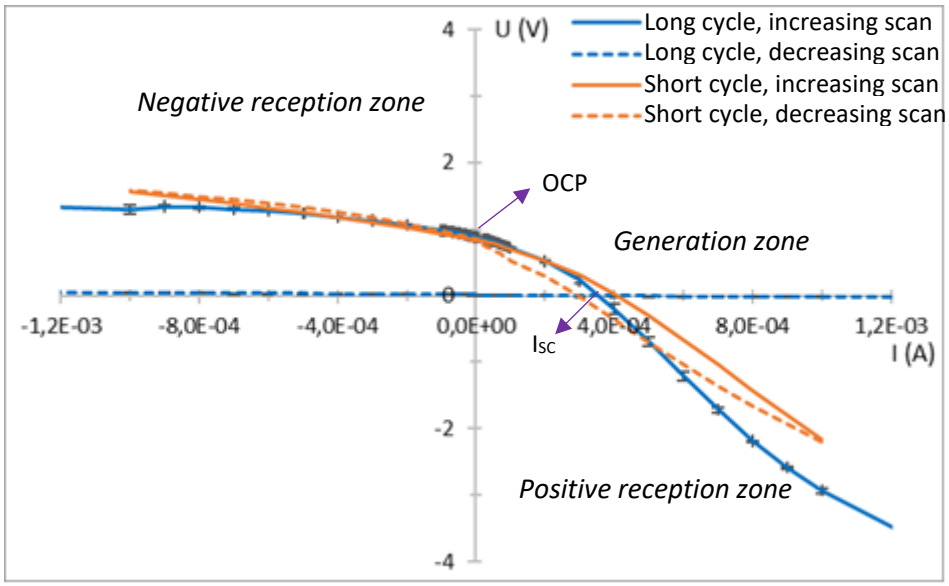

Fig. 10. Comparison of the short cycle polarization curve (-0.1 to 0.1 mA) to the long one (-0.1 to 0.1 A), obtained after 4.5 hours oxidation of Zr with gold deposit, at 850° C. Increasing scan are in solid line and decreasing scan are in dashed line.

In the “positive reception zone" (U<0 and I>0, Fig.11(b) and Fig 3(b)), the imposed external current goes from oxide to metal via the external circuit. Under these conditions, the oxidation current can only be external (I_{Ox}^{Int} =0, I_{Ox} = I_{Ox}^{Ext} from Eq. 11). In this case, the polarization should have been favorable to oxidation of the metal (cathodic polarization of the oxide-side electrode). This zone extends from the short-circuit current (I_{SC} at U=0V, Fig.10) to the maximum value of the applied current (+0.1 mA or +0.1A, depending on short or long cycle).

Finally, the third zone (U>0, I>0, Fig. 11(c)), when the current varies between 0 and I_{SC} value, corresponds to the domain where the oxidizing system behaves in generator mode as an electrochemical cell. The potential measured at I=0A (OCP=0.88V) is close to 1V measured previously over samples without gold deposition (Fig. 6). With the values of I_{SC} ($3.5x10^{-4}$ A) and OCP (0.88V)), it is possible to estimate an approximate value of the total internal resistance of the metal/oxide system operating in generator mode, at the time the polarization curve was measured (4.5 h oxidation), that is equal to 2.5KΩ.

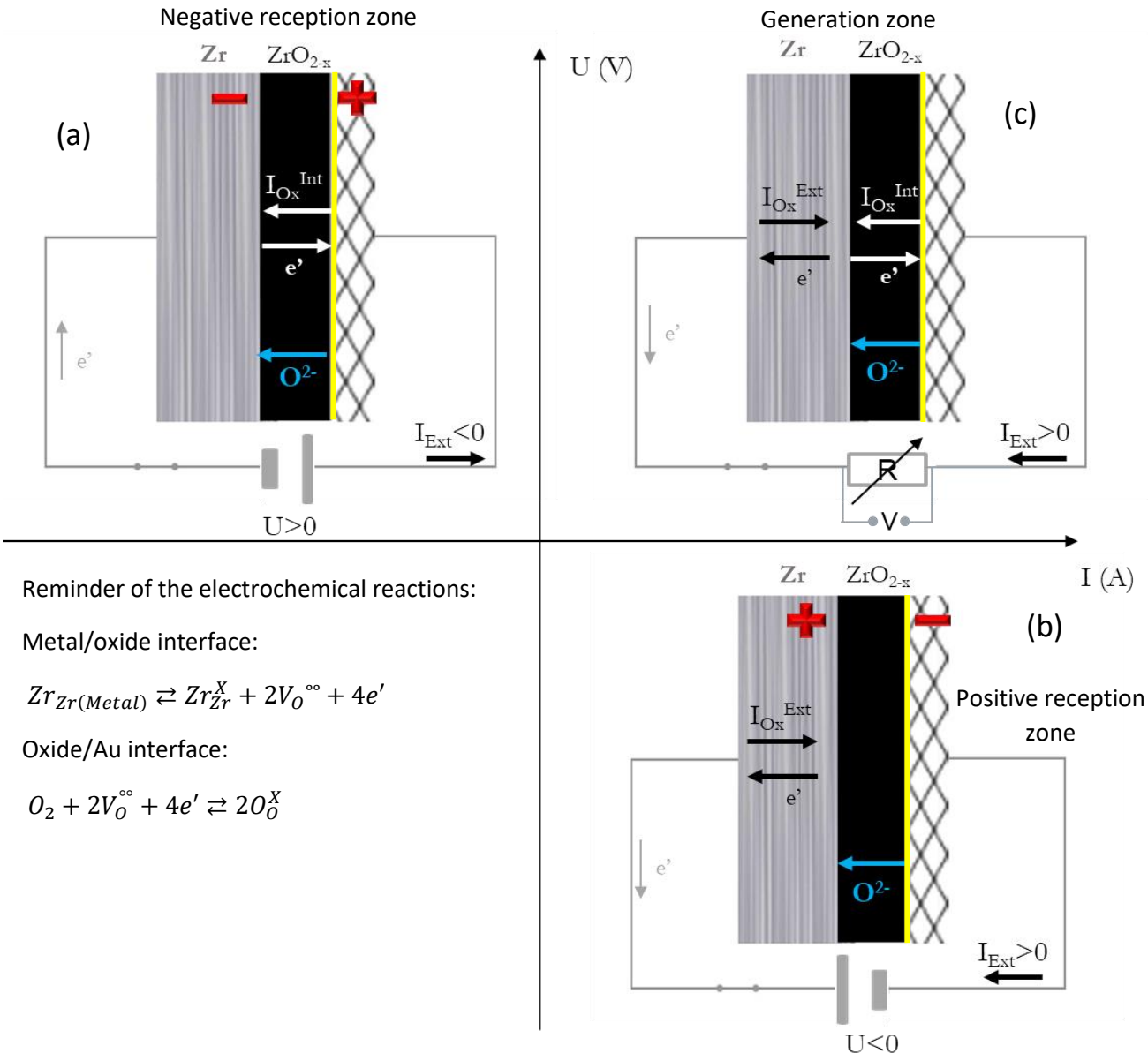

Reminder of the electrochemical reactions:

Metal/oxide interface:

$$Zr_{Zr(Metal)} \rightleftarrows Zr_{Zr}^{X} + 2V_{O}^{\circ\circ} + 4e'$$

Oxide/Au interface:

$$O_2 + 2V_O^{\circ\circ} + 4e' \rightleftarrows 2O_O^X$$

Fig. 11. Interpretation of the three zones of polarization curves.

Fig. 12 shows the evolution of the polarization curve (increasing current scan, long cycle) over the oxidation time. The negative reception zone shows a quasi-linear behavior, where the slope increases continuously with the oxidation time. The maximum potential value obtained in this zone varies from 2 to 4 volts after 3h40 of oxidation.

In the positive reception zone, between the short-circuit current (I_{SC} at U=0) and 8 mA, the potential peak grows with the oxidation time and thus with the increase of the oxide layer thickness. At 15 min oxidation, this peak is weak, but after 3h40 its maximum value reaches up to -6.5±0.4V. Then, at higher current, the potential remains stable around -2V independently on the oxidation times.

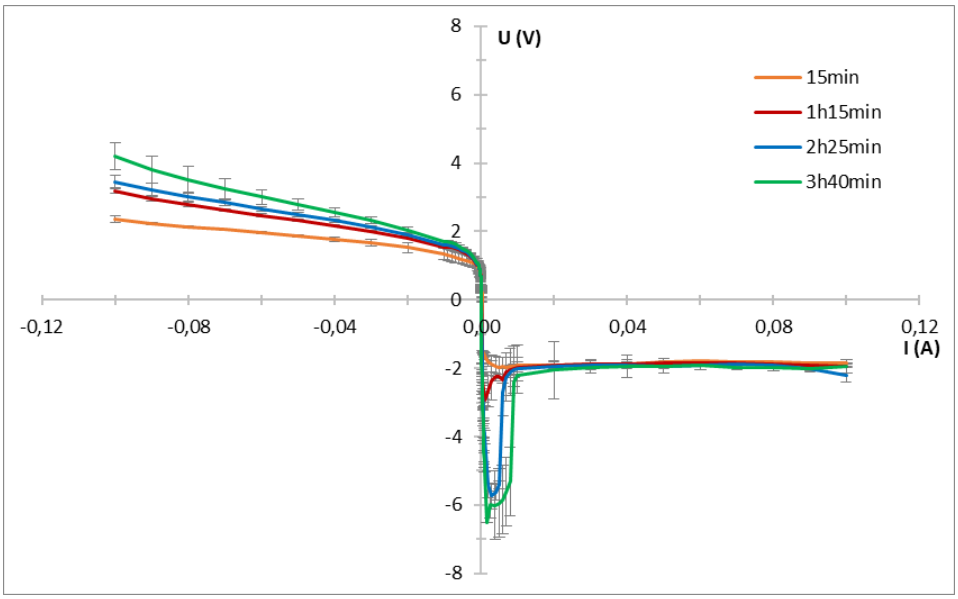

Fig. 12 Polarization curves obtained at four different times during zirconium oxidation at 850°C under He-20% O_2 (increasing current scan).

A zoom of the generation zone is shown in Fig. 13. In this zone, OCP potential remains constant around 1V, regardless of the oxidation time. This is consistent with the experience of continuous OCP measurement during oxidation (Fig. 6). The equivalent resistance of the system (OCP/I_{SC}) increases with the oxidation time, from 0.8 kΩ up to 2.6 kΩ, which is consistent with the progressive growth of the oxide layer.

The short-circuit current decreases over time due to the oxidation rate decrease caused by the growth of the zirconia layer (diffusion regime). Moreover, the contact resistance in the ZrO_2/Au/Pt junction may also vary with the zirconia growth. The short circuit current values obtained from the polarization curves (Fig. 13) are in good agreement to those previously reported in the continuous mode test (Fig. 8).

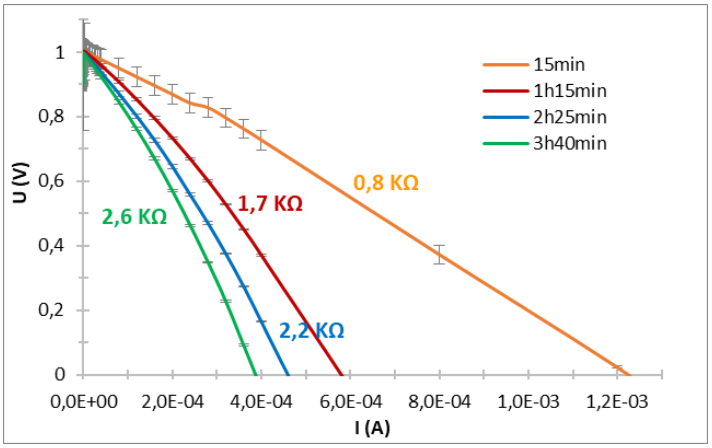

Fig. 13. Zoom of the generation zone of the polarization curves obtained at four different times during zirconium oxidation at 850°C under He-20% O_2 (increasing current scan)

4. Conclusions

Technological developments were performed successfully to investigate oxidation kinetics of metals via thermogravimetric analysis under *in situ* polarization. In parabolic diffusion regime, theoretical ionic oxygen flow calculation indicates that a potential difference of at least 10V across the oxide layer is necessary to influence the oxidation kinetics of zirconium. However, for various experimental reasons concerning the studied system (Metal/oxide/electrode), such a voltage drop through the oxide layer could not be achieved, despite application of high voltage (+/-200 V) to the sample. Without gold layer between the oxide and the electrode, a high contact resistance at the oxide/electrode interface of the order of a few mega ohms is measured. With gold deposit, this contact resistance is reduced by a factor of 1000, but a too high current would be required to reach 10V, leading to heating by Joule effect and modifying the kinetics. Hence, no influence of polarization on zirconium oxidation kinetics could be observed.

Nevertheless, measurements of polarization curves of the metal/oxide/electrode system with gold layer under oxidation showed interesting behavior with hysteresis phenomena. For decreasing current scan from high current (0.1 A, "long cycle"), a quasi-ohmic behavior with a weak overall resistance of the system (a few Ohms) is observed. In other conditions, a non-ohmic behavior with a "generation" zone similar to the one of an electrochemical cell, and two "reception" zones, one positive and one negative were monitored. The open circuit potential (OCP) remains constant at around 1V during oxidation, while the short circuit current (I_{SC}) decreases with time proportionally to the oxidation rate. Modeling of such phenomena with equivalent electrical circuits taking into account both electrochemical properties of the metal/oxide system and the whole system including electrical connections for polarization application is under investigation.

References

[1] Xiaozhu Li, Jun Zhang, Yanwen Yuan, Lingmin Liao, and Chunxu Pan, *Effect of electric field on CuO nanoneedle growth during thermal oxidation and its growth mechanism*, Journal of Applied Physics 024308, 108, (2010) pp. 108, doi.org/10.1063/1.3460635

[2] K. Kawamura, T. Nitobe, H. Kurokawa, M. Ueda, and T. Maruyama, *Effect of Electric Current on Growth of Oxide Scale on Fe–25Cr Alloy for SOFC Interconnect at 1073 K*, Journal of the Electrochemical Society, 159 (3) (2012) pp B259, doi.org/10.1149/2.036203jes

[3] T. Saunders, S. Grasso and M. J. Reece, *Limiting oxidation of ZrB2 by application of an electric field across its oxide scale* , J. of Alloys and Compounds 653 (2015) pp. 629, DOI: 10.1016/j.jallcom.2015.08.112

[4] P. J. Jorgensen, *Effect of an Electric Field on the Oxidation of Zinc,* Journal of Electrochemical Society, Vol 110, (1963) p. 461, doi.org/10.1149/1.2425787

[5] P. J. Jorgensen, *Effect of an Electric Field on Silicon Oxidation*, Journal of Chemical Physics, Vol 37, (1962) p. 874, doi.org/10.1063/1.1733177

[6] J. K. Hinze, PhD thesis « The effect of applied electric fields on diffusion-controlled scaling kinetics», Iowa State University. USA (1973)

[7] I. M. Ritchie, G. H. Scott, and P. J. Fensham, *The effect of an electric field on the oxidation rate of Nickel between 250 and 380°C*, Surface Sci. 19, (1970) p. 230, doi.org/10.1016/0039-6028(70)90121-4

[8] S. K. Roy, V. Ananth, and S. K. Bose, *Oxidation Behavior of Copper at High Temperatures under Two Different Modes of Direct-Current Applications*, Oxidation of Metals, Vol. 43, Nos. 3/4, (1995) p. 185.

[9] G. Lawless and C. A. Lombard, *The Effect of a Static Electric Field on the Oxidation of Certain Metals*, Technical Report AFML-TR-65-412, US Air Force (1966).

[10] H. H. Uhlig and A. E. Brenner, *Effect of Electric Field on Oxidation of Copper*, Acta Metallurgica. Vol 3, (1955) p. 108, doi.org/10.1016/0001-6160(55)90029-8

[11] N. Parkansky, B. Alterkop, S. Goldsmith, R.L. Boxman, Z. Barkay, *Thermal air oxidation of copper in an applied electric field*, Surface and Coatings Technology 146 –147 (2001) 13–18, doi.org/10.1016/S0257-8972(01)01466-9

[12] N. Parkansky, G. Shalev, B. Alterkop, S. Goldsmith, R.L. Boxman, Z. Barkay, L. Glikman, H. Wulff, M. Quaas, *Growth of ZnO nanorods by air annealing of ZnO films with an applied electric field*, Surface & Coatings Technology 201 (2006) 2844–2848, doi.org/10.1016/j.surfcoat.2006.05.032

[13] A V Shishkin, M Ya Sokol and A A Vostrikov, *Effect of electric field on oxide layer structure at zirconium oxidation in H2O, CO2 and H2O/CO2 supercritical fluids*, J. Phys.: Conf. Ser. 1382 012144, 2019, doi.org/10.1088/1742-6596/1382/1/012144

[14] Y. Dali, M. Tupin, P. Bossis, M. Pijolat, Y. Wouters and F. Jomard, *Corrosion kinetics under high pressure of steam of pure zirconium and zirconium alloys followed by in situ thermogravimetry*, J. of Nuclear Materials, Vol 426 (2012) p. 148, doi.org/10.1016/j.jnucmat.2012.03.030

[15] M. Tupin, M. Pijolat, F. Valdivieso, M. Soustelle, A. Frichet and P. Barberis, *Differences in reactivity of oxide growth during the oxidation of Zircaloy-4 in water vapour before and after the kinetic transition*, J. of Nuclear Materials, Vol 317 (2003) p. 130, doi.org/10.1016/S0022-3115(02)01704-X

[16] I. Idarraga, M. Mermoux, C. Duriez, A. Crisci and J.P. Mardon, *Raman investigation of pre- and post-breakaway oxide scales formed on Zircaloy-4 and M5® in air at high temperature*, J. of Nuclear Materials, Vol 421 (2012) p. 160, doi.org/10.1016/j.jnucmat.2011.11.071

[17] M. Lasserre, V. Peres, M. Pijolat, O, Coindreau, C. Duriez and J.P. Mardon, *Modelling of Zircaloy-4 accelerated degradation kinetics in nitrogen–oxygen mixtures at 850 °C*, J. of Nuclear Materials, Vol 462 (2015) p. 221, doi.org/10.1016/j.jnucmat.2015.03.052

[18] M. Steinbrück, *Oxidation of Zirconium Alloys in Oxygen at High Temperatures up to 1600°C*. *Oxid Met* **70,** 317–329 (2008). https://doi.org/10.1007/s11085-008-9124-z

[19] A.T Fromhold, *Parabolic oxidation of metals in homogeneous electric fields,* J. Phys. Chem. Solids, Vol. 33 (1972), pp. 95- 120.

[20] B. Cox, Some thoughts on the mechanisms of in-reactor corrosion of zirconium alloys, Journal of Nuclear Materials, Vol. 336 (2005) p. 331, doi.org/10.1016/j.jnucmat.2004.09.029

[21] V.V. Kharton et al., *Research on the electrochemistry of oxygen ion conductors in the former Soviet Union. I. ZrO2-based ceramic materials*, Journal of Solid State Electrochem. Vol 3 (1999), p. 61, doi.org/10.1007/s100080050131

[22] M. de Ridder et al., *Oxygen exchange and diffusion in the near surface of pure and modified yttria-stabilised zirconia*, Solid State Ionics, Vol 158 (2003) p. 67, doi.org/10.1016/S0167-2738(02)00759-2

[23] P.S. Manning, J.D. Sirman, R.A. De Souza, J. Kilner, *The kinetics of oxygen transport in 9.5 mol % single crystal yttria stabilised zirconia*, Solid State Ionics, Vol 100 (1997) p. 1, doi.org/10.1016/S0167-2738(97)00345-7

[24] N. Sakai et al., *Transport properties of ceria–zirconia–yttria solid solutions* $\{(CeO2)_x(ZrO2)_{1-x}\}_{1-y}(YO1.5)_y$ *(x = 0–1, y = 0.2, 0.35)*, Journal of Alloys and Compounds (2006) 408-412, p. 503, doi.org/10.1016/j.jallcom.2004.12.088

[25] A. Kasperski, C. Duriez and M. Mermoux, *Combined Raman Imaging and 18O Tracer Analysis for the Study of Zircaloy-4 High-Temperature Oxidation in Spent Fuel Pool Accident*, In STP1597-EB Zirconium in the Nuclear Industry: 18th International Symposium. West Conshohocken, PA: ASTM International (2018) pp. 1059-1092, doi.org/10.1520/STP159720160037

[26] X. Ma, C. Toffolon-Masclet, T. Guilbert, D. Hamon, and J.C. Brachet, *Oxidation kinetics and oxygen diffusion in low-tin Zircaloy-4 up to 1523 K*, Journal of Nuclear Materials, Vol. 377, No. 2 (2008) p. 359-369, doi.org/10.1016/j.jnucmat.2008.03.012

[27] M. Howlader et al., *In situ measurement of electrical conductivity of Zircaloy oxides and their formation mechanism under electron irradiation*, Journal of Nuclear Materials, Vol. 265, (1999) p. 100-107, doi.org/10.1016/S0022-3115(98)00609-6